JOURNAL OF APPLIED PHYSICS 115, 224305 (2014)

Fracture toughness of the sidewall fluorinated carbon nanotube-epoxy interface

Yogeeswaran Ganesan,[1] Hossein Salahshoor,[2] Cheng Peng,[1] Valery Khabashesku,[3] Jiangnan Zhang,[1] Avery Cate,[1] Nima Rahbar,[2,a)] and Jun Lou[1,a)]
[1]*Department of Materials Science and NanoEngineering, Rice University, Houston, Texas 77005, USA*
[2]*Department of Civil and Environmental Engineering and Department of Mechanical Engineering, Worcester Polytechnic Institute, Worcester, Massachusetts 01609, USA*
[3]*Department of Chemical and Biomolecular Engineering, University of Houston, Houston, Texas 77204, USA*

(Received 13 March 2014; accepted 25 May 2014; published online 12 June 2014)

The effects of carbon nanotube (CNT) sidewall fluorination on the interface toughness of the CNT epoxy interface have been comprehensively investigated. Nanoscale quantitative single-CNT pull-out experiments have been conducted on individual fluorinated CNTs embedded in an epoxy matrix, *in situ*, within a scanning electron microscope (SEM) using an InSEM® nanoindenter assisted micro-device. Equations that were derived using a continuum fracture mechanics model have been applied to compute the interfacial fracture energy values for the system. The interfacial fracture energy values have also been independently computed by modeling the fluorinated graphene-epoxy interface using molecular dynamics simulations and adhesion mechanisms have been proposed. © *2014 AIP Publishing LLC*. [http://dx.doi.org/10.1063/1.4881882]

I. INTRODUCTION

One of the most promising applications for carbon nanotubes (CNTs) is as reinforcements for high strength/stiffness/toughness composites because their mechanical properties are considerably better than those of conventional fibrous materials. In fact, significant improvements in the mechanical properties have been observed upon nanotube addition to thermoplastic and elastomeric matrices. For example, an 80% improvement in tensile modulus was observed upon 1% CNT addition to poly-(vinyl alcohol) (PVA).[1] In another work, a 3-fold increase in the Young's modulus was obtained upon addition of single-wall carbon nanotubes (SWNT) (1 wt. %) into room temperature vulcanizing silicone rubber matrix.[2] However, the reinforcement of epoxy resins by carbon nanotubes is generally considered problematic and only marginal improvements or even a decrease the in composite modulus have been observed, after the addition of CNTs.[3]

This is because (a) nanotubes tend to remain as entangled agglomerates within epoxy and homogeneous dispersions are not easily obtained. (b) The CNTs do not bond with the matrix and are typically pulled out from the matrix upon application of small loads i.e. they play a limited reinforcement role. Additionally, (c) processing difficulties that arise due to the significant increases in viscosity, caused by the addition of nanotubes into epoxy, result in inferior composite specimens.[4]

The mechanical properties of a CNT reinforced polymer composite can, in theory, be improved by the addition of functional groups, such as carboxylic acid, fluorine, or amino moieties to the surface of the CNTs.[4–8] Functional groups can promote CNT dispersion within a polymer matrix and, more importantly, improve interfacial adhesion by forming chemical or physical bonds with polymer matrices. Several approaches to achieve the functionalization of CNTs have been developed, in both molecular and supramolecular chemistry, including defect functionalization, covalent functionalization of the side-walls, non-covalent exohedral functionalization, and endohedral functionalization.[9] Sidewall fluorination is one such functionalization strategy that can not only improve CNT dispersion considerably but also be easily substituted with more complex addends, opening the way to more complex chemical functionalization of nanotubes for improved interactions with various matrix materials.[10] With regard to epoxy matrices, sidewall fluorination is of particular importance, since while fluorine on CNT sidewalls cannot itself bond to epoxy, it is capable of reacting with amine based curing agents commonly used to harden epoxy and establishing covalent linkages with the matrix.[4]

In order to gain an understanding of and accurately assess the effectiveness of any CNT surface functionalization technique, it is critical to reliably characterize the mechanical properties of the resulting CNT-matrix interface. Owing to the small size of CNTs, conducting any direct nanoscale mechanical tests on them can be challenging owing to the magnitude of the forces and displacements that must be applied and measured. Indirect analysis techniques, such as macro-scale composite specimen testing and strain induced Raman shift measurements, have been found to be extremely convenient and thus commonly used to assess the strength and load transfer efficiency of CNT-matrix interfaces,[1,11,12] although there have been a handful of reports that discuss nanoscale single CNT/CNF pullout.[13–17] Implementation of a single fiber pull-out analysis is considered extremely desirable within the composite science community, since few assumptions need be made when interpreting experimental data and because they provide extremely accurate and reliable results. The single fiber pull-out experiment is a quantitative method for the localized characterization of interfaces

[a)]Authors to whom correspondence should be addressed. Electronic addresses: nrahbar@wpi.edu and jlou@rice.edu

and involves the application (and measurement) of a precise load to eject an individual fiber from a matrix. In addition to the interfacial bond strength and interfacial toughness, other interfacial properties such as the matrix shrinkage pressure on the filler, the interfacial shear stress (IFSS), and the work done in pulling out the filler from the matrix, can be determined by performing a single fiber pullout experiment. The latter is of particular importance, since the fracture toughness of a fibrous composite depends largely on the fiber pull-out process during failure.[18]

In the past, we had reported on the development of a novel nanoindenter assisted technique that could be used for performing *in situ* nanomechanical testing on 1D nanomaterials.[19,20] We also reported on the usage of the technique to perform 15 successful single fiber pullout experiments, which allowed us to measure the fracture energy, G_c, of the pristine multi-walled carbon nanotube (MWNT)-Epon 828 interface.[21] Here, we discuss the results of a set of 13 single fluorinated MWNT pull-out experiments from an Epon-828^{TM} matrix, which were performed within a scanning electron microscope (SEM) by employing the same technique. Additionally, the results of molecular dynamics (MD) simulations to independently assess the adhesion between fluorinated graphene and Epon-828^{TM}, considered to be analogous to the fluorinated MWNT-Epon-828^{TM} system, will be discussed.

II. RESULTS AND DISCUSSION

A. Single fiber pullout experiments

Novel micro-devices, which functioned on the basis of a spring-like "push-pull" mechanism, were used to conduct the pullout of individual fluorinated MWNTs from epoxy matrices.[19] Loading of the pull-out specimen was achieved by the usage of a nanoindenter which applied a displacement to the top shuttle of the devices, which four sets of inclined symmetrical beams transformed into a two dimensional translation of the central section. The procedure ensured that the stress applied on the pullout specimen, positioned across a gap in the central section, is purely axial. MWNT fluorination, single fiber pullout specimen preparation (see Fig. 1) and the pullout experimental procedure are described in detail in the Experimental section. The pullout of MWNTs from the surrounding matrix first involved an increase in the applied load, while the nanotubes remained in full contact with the polymer matrix (see Figs. 2(a) and 2(b)). When the applied load reached a critical value, tens of μN in this case, the MWNTs debonded entirely from the epoxy matrix (Fig. 2(c)). This full debonding instantaneously resulted in a sharp drop in the recorded load to near zero values, a phenomenon that was expected to occur since the forces required to overcome the frictional interaction between the surface of a smooth MWNT and epoxy were assumed to be negligible. The MWNTs subsequently pulled out of the epoxy matrix at negligible applied loads (Fig. 2(d)). Fig. 3 shows representative single fiber pullout load-extension curves that were extracted from their corresponding nanoindenter force vs. displacement curves, using a simple response subtraction procedure.[20,21]

Four types of failure are generally known to occur during a typical single-fiber pullout test. These include (i) specimen (nanotube embedded in matrix) failure due to matrix failure away from the fiber-matrix interface, (ii) specimen failure by fiber fracture along the external free length of the fiber, (iii) partial debonding followed by specimen failure due to fiber fracture along the embedded length of the fiber,

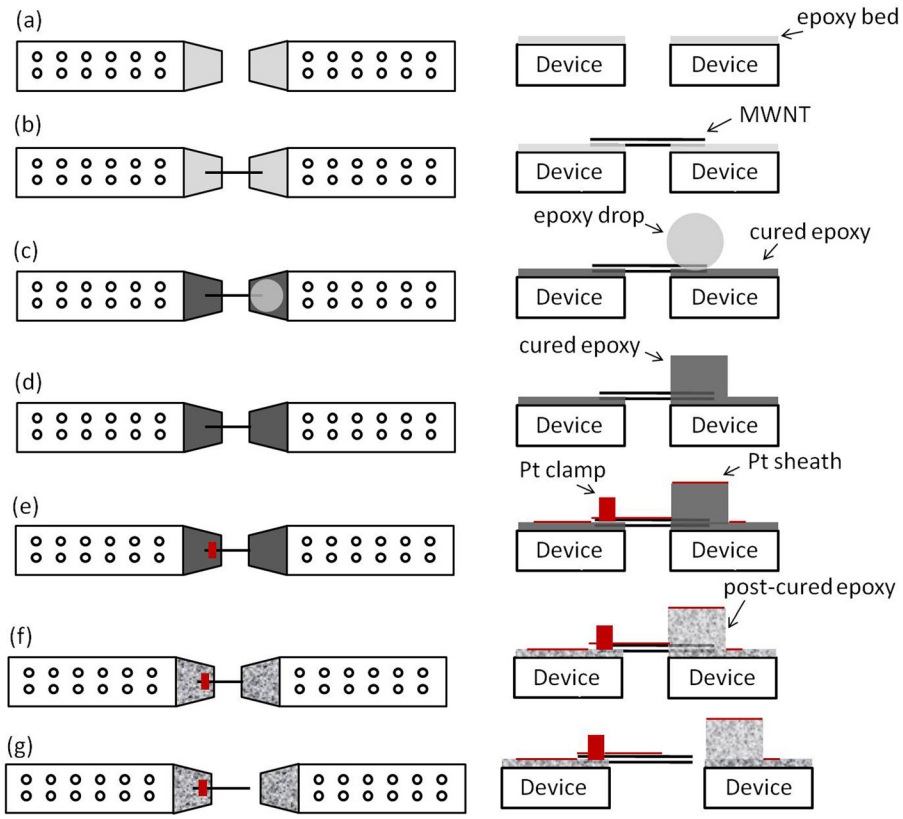

FIG. 1. Sample preparation procedure; for each step undertaken, the top and side views of the sample stage shuttles are shown side by side. (a) The ends of the sample stage shuttles are first coated with a thin layer of the epoxy, (b) an individual MWNT is placed across the gap (embedment depth is ascertained at this juncture), (c) a single droplet of epoxy is dropped onto one of the sample stage shuttles, (d) the droplet of epoxy upon curing at room temperature embeds one end of the MWNT, (e) the MWNT is clamped close to the other end by EBID Pt; this inadvertently results in the sheathing of the exposed part of the MWNT with a thin layer of Pt, (f) the specimen is post cured and finally (g) pullout experiment is performed.

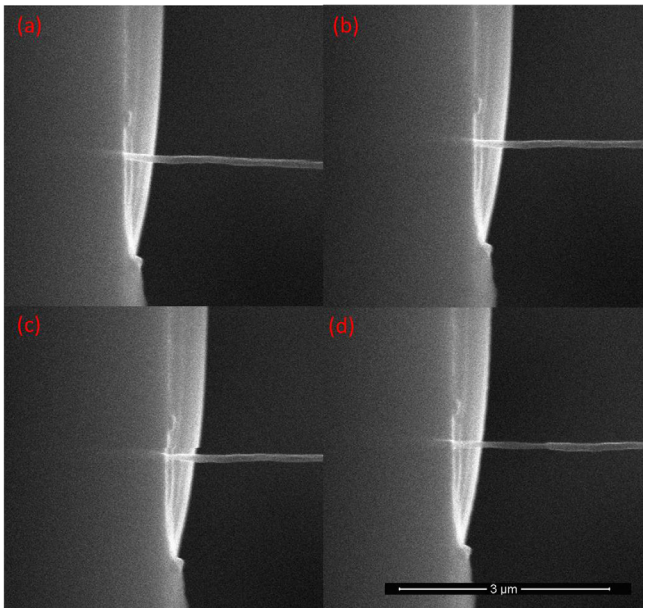

FIG. 2. SEM snapshots show a single fluorinated MWNT as it pulls out of an epoxy matrix, at (a) t = 0, (b) t = , 8(c) t = 16, and (d) t = 144 s, during a typical pullout experiment. The pullout experiment was conducted at an indenter displacement rate of 10 nm/s. Note that in (c) and (d) the section of the nanotube that was not embedded in the epoxy matrix is laterally wider compared to the embedded section, owing to the presence of a sheath of Pt deposited during MWNT clamping step.

and (iv) specimen failure due to complete debonding and extraction of the debonded fiber from the matrix. The first three types of failure represent unsuccessful pullout tests and data from specimens that exhibit these types of failure are not included in pullout analyses. With regard to MWNT pullout from epoxy, the first three types of failure were not observed during the experiments. SEM images of embedded portions of MWNTs post successful pullout showed no evidence of polymer residues on the nanotube surface, indicating that failure occurred at the MWNT-epoxy boundary and not within the epoxy matrix. Also nanotube embedment depth verification conducted post pullout (the embedment depth was initially ascertained prior to complete embedment) ensured no MWNT breakage occurred within matrix during the pullout experiments. Unsuccessful experiments were usually the result of the hitherto undocumented failure mode (v), i.e., failure of the electron beam induced deposition (EBID) platinum clamps that attached one end of the nanotubes to the devices and subsequent detachment of nanotube from device occurring at the platinum deposition sites. 13 successful pullout experiments, with embedment values ranging from 3.13 nm to 6.01 μm, were conducted (Table I) and their load vs. extension traces extracted were used to ascertain the interfacial properties of the composite system. Due to the difficulties associated with MWNT embedment depth control, it was not possible to obtain any data corresponding to embedment depths lower than 3 μm. It was also not possible to conduct any successful pullout experiments on fluorinated MWNTs with embedment depths greater than 6 μm, owing to the weak nature of the EBID Pt clamps (MWNTs with embedment depths greater than 6 μm in the epoxy matrix detached from devices at Pt deposition sites during pullout experiment). Fig. 4 shows the maximum MWNT pull-out force measured on the 13 samples representing a reasonably wide range of embedments. As expected for single fiber pull-out experiments, the data exhibit considerable scatter. Experiments conducted on pristine MWNTs[21] and those conducted by others in the past on the MWNT-polyethene-butene system, revealed a similar scatter in the data.[14] It is postulated that the scatter arises partially due to the fact that minor variations that occur during specimen preparation have a substantial effect on the values of maximum pullout load obtained. The average IFSS, τ_{avg}, a frequently quoted parameter used by researchers when analyzing the results of single fiber pullout experiments, was calculated using the following equation:

$$\tau_{avg} = \frac{P}{2\pi r l}, \tag{1}$$

where P is the experimentally measured maximum pull-out load, r is the MWNT radius, and l is the embedment depth. The fluorinated MWNTs showed a τ_{avg} that decreased as

TABLE I. Interfacial properties ascertained from single sidewall fluorinated MWNT pullout experiments. For cases in which the nature of the load-extension response was non-linear or ambiguous, the G_c values could not be calculated. (N.A. = not applicable).

Embedment depth (μm)	MWNT outer diameter (nm)	Maximum pullout load, P (μN)	Average interfacial shear strength, τ_{avg} (MPa)	Nature of load-extension response	Interfacial fracture energy, G_c (J/m^2)
3.13	64	11.51	18.27	Linear	0.784
3.35	76	27.31	34.03	Linear	2.617
3.36	91	11.73	12.28	Linear	0.287
3.44	78	10.54	12.51	Linear	0.365
3.46	79	29.19	34.05	Linear	2.704
3.52	91	28.02	27.86	Linear	1.624
3.58	89	15.84	15.85	Linear	0.557
4.15	107	21.70	15.48	Linear	0.596
5.47	99	17.24	10.16	Not clear	N.A.
5.65	114	37.67	18.67	Linear	1.501
5.74	78	23.92	17.12	Linear	1.916
6.00	91	23.60	13.82	Non-linear	N.A.
6.01	59	19.78	17.70	Non-linear	N.A.

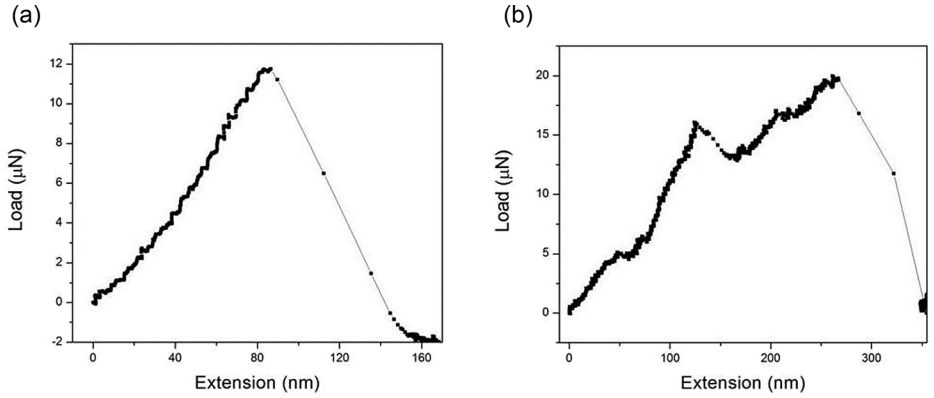

FIG. 3. Representative load-extension curves for (a) a fluorinated MWNT specimen with a small embedment depth (3.36 μm) and (b) a fluorinated MWNT specimen with large embedment depth (6.01 μm).

embedment depth increased a behavior consistent with shear-lag theory,[15] although there were multiple outliers at shorter embedment depths. The average value of τ_{avg}, for the fluorinated MWNT/Epon 828 interface (19.8 ± 7.78 MPa), was found to be larger than that for the pristine MWNT/Epon 828 interface (6.24 ± 3.6 MPa),[21] thus demonstrating the sensitivity of interfacial adhesion to MWNT surface treatments such as sidewall fluorination. These values are comparable to those reported for the MWNT-Poxipol™ interface (~22.6 MPa),[15] the double walled CNT-PMMA interface,[17] the pristine graphitized vapor grown carbon nanofiber epoxy interface (~66 MPa),[13] and the MWNT-polyethene-butene interface (~15 MPa),[14] but an order of magnitude lower than those reported for the MWNT-polyurethane interface (~500 MPa),[22] carbon nanofiber-Epikote™ interface (~170 MPa),[16] and the oxidatively functionalized vapor grown carbon nanofiber-epoxy interface (~189 MPa).[13]

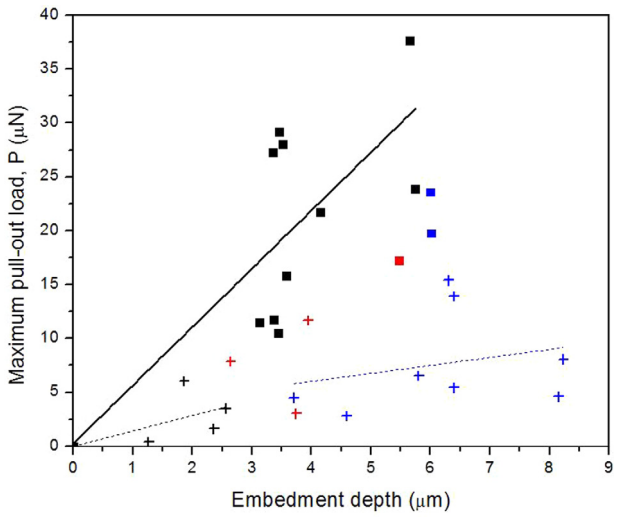

FIG. 4. Maximum pullout load, P, versus nanotube embedment depth, plotted for both fluorinated and pristine[21] Mitsui™ MWNT pullout. The black plus signs (for pristine) and black solid squares (for fluorinated MWNTs) indicate points corresponding to embedments that exhibited a linear pull-out load-extension response. The blue plus signs (for pristine) and blue solid squares (for fluorinated MWNTs) indicate points corresponding to deep embedments that exhibited a non-linear pull-out load-extension response. The red plus signs (for pristine) and red solid squares (for fluorinated MWNTs) indicate points corresponding to embedments that did not exhibit a clearly linear or non-linear pull-out load-extension response. Also shown are the linear fits that were applied for the points indicated by black plus signs and blue plus signs viz. the black dotted line and the blue dotted line, respectively; their point of convergence was used to determine l_{th}, and its corresponding maximum pull-out force value P (asymptotic), for the pristine MWNT-epoxy interface. A similar linear fit, indicated by the black solid line, was applied for points indicated by black solid squares but l_{th} could not be computed, in this case, owing to the paucity of points, indicated by blue solid squares, corresponding to embedments that exhibited a non-linear pull-out load-extension response.

Fluorinated MWNTs with short embedment depths ($l \ll 6\ \mu$m) exhibited a linear pre-peak response (Fig. 3(a)) and were thus assumed to have pulled out as a result of catastrophic (unstable) propagation of an initiated interface crack, i.e., crack growth and complete debonding occurred catastrophically as soon as the critical load for crack propagation, P_c was attained ($P = P_c$ in these cases). Deep embedments ($l \sim 6\ \mu$m), however, produced nonlinear load-extension responses prior to peak load (Fig. 3(b)) and pull-out was assumed to have not occurred when applied load equaled P_c; crack growth was assumed to have proceeded in stable fashion post attainment of P_c, requiring continued increase in the applied load ($P > P_c$ in these cases, since frictional energy dissipation would occur along the debonded length). These results were found to be consistent with predictions of continuum fracture mechanics models and were thus analysed via the usage of the approximate fracture mechanics model developed by Jiang and Penn.[23] Neglecting the effects of matrix compression, a reasonable assumption since the pullout specimens were cured at room temperature, and assigning a zero value of friction coefficient to the analytical formulas in Ref. 23 lead to the following formula relating P_c, the Young's modulus of the fiber (matrix), E_f (E_m), the Poisson's ratio of the matrix, υ_m, the radial distance from the fiber axis at which the shear stress in the matrix reduces to zero, R, the embedment depth, l, the initial crack length at the interface, a and the MWNT radius, r

$$P_c = \frac{2\pi r\sqrt{rE_fG_c}}{\sqrt{1+\mathrm{csch}^2\left(n\frac{l-a}{r}\right)}}, \tag{2}$$

where n is a utility constant defined as

$$n = \sqrt{\frac{E_m}{E_f(1+\upsilon_m)\ln\frac{R}{r}}}.$$

It is important to acknowledge, at this juncture, that Eq. (2) cannot just be solved to ascertain G_c using any experimental maximum pullout load, P, value. P values associated with

deep embedments, i.e., those displaying non-linear pullout load-extension curves, can be considered to be equal to the load required to debond the MWNT from the epoxy plus an amount of energy dissipated by frictional effects between the MWNT and the epoxy during stable crack extension, over the debonded length. Equation (2) is a simplification that hinges on the elimination of frictional energy dissipation terms and is only valid for interfacial failure that occurs in a catastrophic fashion. P values associated with very short embedments must also not be used to calculate G_c as they are susceptible to errors resulting from the presence of initial cracks at the interface (formed during specimen preparation or handling, initial cracks that are a large fraction of the embedment depth can reduce the value of P substantially). In the ideal scenario, the asymptotic P value ($P = P_c$), defined as the load at which the pullout load-extension curves change from exhibiting a linear to a nonlinear behavior, would result in the most accurate estimate of G_c; this load value and its corresponding embedment depth value, l_{th}, can be picked off a maximum pull-out load versus embedment depth plot as the load at which a distinct slope change occurs.[23] The aforementioned technique was adopted successfully earlier, to accurately estimate the G_c values for the pristine MWNT-epoxy interface.[21] However, in the case of the fluorinated MWNT-epoxy system, data were not available to plot maximum pull-out load versus embedment depth over a sufficiently wide range of embedment depths. Note that only two points on plot shown in Fig. 4 and Table I correspond to non-linear load vs. extension curves for fluorinated MWNT pullout, and a clear transition from linear to a nonlinear pullout load-extension curve behavior was not observed during our experiments. Thus, the entire set of measured values of maximum pull-out force corresponding to pull-outs characterized by a linear load-extension response was used to compute the value of interfacial fracture energy G_c for the fluorinated Mitsui^{TM} MWNT-Epon 828 interface using Eq. (2) (shown in Table I).

With regard to the G_c calculations using Eq. (2), it must be mentioned that the average Young's modulus value for the fluorinated Mitsui^{TM} MWNT specimens was not obtained directly by performing tensile tests on the nanotubes. Instead, the magnitude of the reduction in MWNT Young's Modulus brought about by fluorination was estimated based on tensile experiments conducted on pristine and fluorinated DLI-CVD (Direct Liquid Injection-Chemical Vapor Deposition) MWNTs.[24] In the case of the DLI-CVD MWNTs, a 35% reduction in the Young's Modulus was observed upon fluorination (average apparent Young's Moduli for pristine DLI-CVD MWNTs was found to be equal to 54.3 GPa; this value reduced to about 35.3 GPa upon sidewall fluorination). Pristine Mitsui^{TM} MWNTs, whose Young's modulus was measured by conducting tensile experiments and found to be equal to 200 GPa, were thus assumed to have degraded similarly and hence their Young's Modulus value was set to 130.16 GPa. The modulus of unreinforced Epon 828 (mixed with Epikure^{TM} 3200 in a 10:1 ratio) resin was measured using tension experiments conducted on dog-bone shaped resin specimens. The average value E_m was found to be 1.099 GPa. The Poisson's ratio of the resin was set equal to 0.33.[25]

In the nanotube pullout configuration studied the R/r parameter could not be determined. By assuming a stress transfer parameter R/r value ranging from 2 (a value typical for weak interfaces) to 9 (a value that would be typical for a strong interface) and a zero value for the initial crack length at the interface, Eq. (2) provided a set of 10 interfacial fracture energy values for the fluorinated MWNT-Epon 828 interface, within the range of 0.29–2.70 J/m^2. Note that the choice of the value of the stress transfer parameter R/r does not significantly affect the value of G_c. The G_c values were found to be about one order of magnitude higher than that for the pristine MWNT/Epon 828 interface, viz., 0.05–0.25 J/m^2 (Ref. 21) and thus comparable to the values reported for nanotube pullout from a polyethylene-butene matrix (4–70 J/m^2),[14] pristine graphitized and oxidatively functionalized vapor grown carbon nanofibers from an epoxy matrix (0.65 and 3.3 J/m^2, respectively)[13] and the double walled CNT-PMMA interface (0.13–0.23 J/m^2).[17] The values were still, however, approximately one order of magnitude lower than that for engineered composite materials (16–34 J/m^2).[26]

B. MD simulations

Ab initio MD simulations performed to study the nanomechanical properties of pristine graphene, Epon 828^{TM} cured with aminoethylpiperazine (AEP, commercially known as Epikure 3200^{TM}) and adhesion at the pristine graphene-Epon 828 (cured with AEP) interface have been discussed in detail earlier.[27] The interfacial fracture energy for the system was computed to be about 0.203 J/m^2, a value that was found to be in good agreement with the results of the pristine MWNT pullout experiments conducted from the Epon 828^{TM} matrix.[21] Fig. 5 shows the evolution of a MD simulation model consisting of a fluorinated graphene sheet in contact with Epon 828^{TM} (mixed with Epikure 3200^{TM}) at 4 different stages, when subjected to the same curing conditions that the MWNT pullout specimens were subjected to. The degree of sidewall fluorination chosen for the simulations was 25%, a value that essentially mimicked that of the fluorinated MWNTs used in the pullout experiments. Interfacial fracture energy was assumed to be equal to the work of adhesion at nanoscale, viz., the interaction energy per unit area between the two materials. The interaction energy is the difference between the total energy of the system and the energies of the individual entities

$$E_{Interaction} = E_{Total} - (E_{Graphene} + E_{Epoxy}). \quad (3)$$

Therefore, in order to calculate the interaction energy, the energy of the whole system, post attainment of equilibrium state, was first computed. The interaction energy was then computed by subtracting the summation of the energies of each layer, which were computed separately, from the total energy. Table II shows the energy values computed using the MD simulations. The negative sign of the interaction energy implied that the two layers adhered to each other. The calculated interfacial fracture energy was found about 2.7 J/m^2, a value that was comparable to those obtained from the single MWNT pullout experiment results and in fact, equal to the maximum value observed. In addition, the waviness/roughness

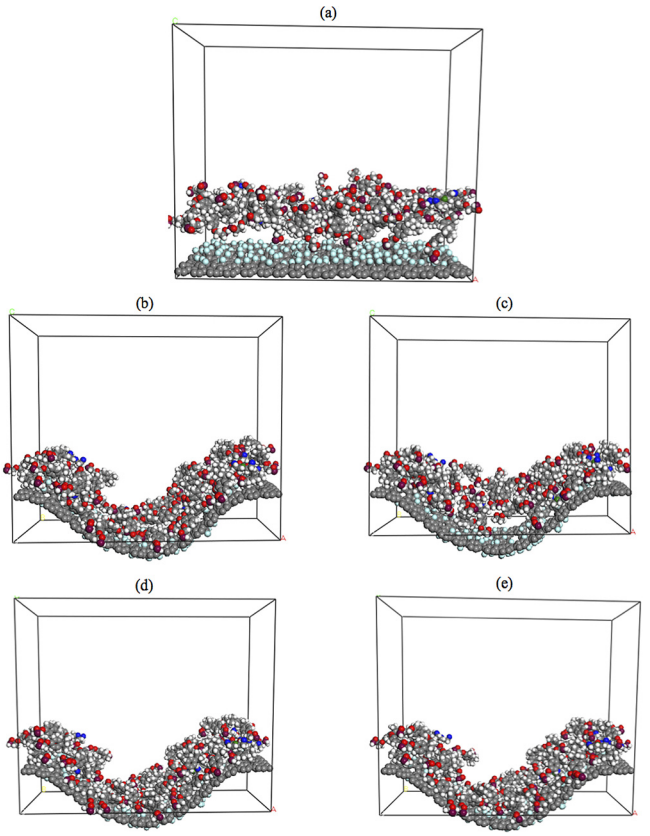

FIG. 5. In order to study the adhesion mechanisms, fluorinated graphene (F and C atoms represented by light blue circles and gray circles respectively) and a DGEBA (Epon-828^{TM}) + AEP (Epicure 3200^{TM}) mixture (molecules represented by open circles, dark blue circles, gray circles, and red circles) were built in contact in a large unit cell with a vacuum slab above the epoxy layer. MD simulations results at different stages of curing process are shown here: (a) Initial system, (b) after raising temperature to 358 K, (c) after cooling to 338 K, (d) after cooling to 318 K, and (e) after bringing it back to room temperature (final equilibrium state).

of the fluorinated graphene sheet at the pristine graphene/epoxy interface was also computed using the MD simulation model. Adhesion of a graphene sheet to its substrate is known to cause higher roughness/waviness and corrugation in the graphene sheet, with stronger adhesion resulting in a higher magnitude of sheet corrugation. The waviness of pristine graphene at the pristine graphene-epoxy interface was computed earlier and found to be about 3.2 Å.[27] In this study, the waviness of fluorinated graphene at the fluorinated graphene-epoxy interface was computed to be about 7.5 Å, thus indicating that stronger adhesive forces existed at the fluorinated graphene-epoxy interface compared to the pristine graphene-epoxy interface. Note that in the case of both pristine and fluorinated graphene, the sheets were assumed to be atomically flat prior to contact with epoxy.

TABLE II. Energy values, derived using the MD simulation model shown in Figure 5, at the final equilibrated state (at room temperature).

Energy terms	Energy (kcal/mol)
Total energy	185.8×10^3
Epoxy energy	178.4×10^3
Fluorinated graphene energy	15.5×10^3
Interaction energy	-8.1×10^3

From our past results, we inferred that weak van der Waal's forces were primarily responsible for the weak interfacial adhesion at the pristine MWNT-Epon 828 interface.[21] However, as mentioned earlier, fluorine on the sidewalls of fluorinated MWNTs has been known to be readily displaced by alkylidene amino groups, such as those present in AEP. Reports suggest that fluorinated CNTs can react *in situ* with amine curing agents (such as Epikure 3200^{TM}) during a high temperature curing processes (130 °C and above), thus establishing covalent linkages with an epoxy matrix.[4] Since the pullout specimens were room temperature cured and subsequently post cured at 80 °C, it was unlikely that any significant covalent bonding occurred between the fluorinated MWNTs and the epoxy matrix. Any enhancement in the polymer's chain wrapping ability, upon MWNT fluorination, was also unlikely owing to the large diameters of the MWNTs. Thus, the improvement in the interfacial adhesion was assumed to have occurred partly due to an increase in the surface roughness of the MWNTs brought about by fluorination. Surface topography analyses conducted on the Mitsui^{TM} MWNTs, before and after the fluorination process, using an AFM (atomic force microscope) showed that the surface root mean square roughness of the tubes increased from 4 to 6 Å. Another key factor that presumably contributed significantly to the improvement in interfacial adhesion is the existence of strong electrostatic interactions between fluorine, a highly electronegative element, on the MWNT surface and the epoxy matrix. It is worth noting that in a separate effort, macro-scale tensile tests were conducted on dog-bone shaped fluorinated MWNT-epoxy composite specimens. 0.5%, by weight, sidewall fluorinated Mitsui^{TM} MWNTs were incorporated into the Epon 828 matrix (sample preparation conditions mimicked those used for preparing pullout specimens) and the mechanical properties of the composites were studied. The reinforcing effect of the MWNTs was found to be considerable, with a 17% increase in the Young's modulus effected upon their addition (no such increase was observed upon addition of pristine Mitsui^{TM} MWNTs) thus corroborating the conclusion that an improvement in adhesion at the MWNT-Epon 828 interface does actually occur upon MWNT fluorination which translates to improved mechanical properties for the composite observable at the macroscale.

III. EXPERIMENTAL

The pull-out specimens used in this study comprised individual fluorinated MWNTs embedded in Epon 828 epoxy films covering certain sections of the sample stage shuttles of novel micro-devices (Fig. 1). A mixture of 10% elemental fluorine and 90% helium was used as the fluorinating agent for pristine MWNTs (Mitsui Corp., Japan, lot no. 05072001K28). This mixture along with additional helium gas feed was passed through a temperature controlled Monel flow reactor, held at 160 °C, containing the nanotube sample. A 4% increase in the weight of the samples occurred after fluorination. X ray photoelectron spectroscopy conducted on the MWNTs showed the C:F ratio on the surface of the MWNTs to be 77.9:22.1.

For pullout specimen preparation, a portion of each sample stage shuttle was first coated with a thin layer of 10:1 epoxy, Epon 828 (chemical name: diglycidyl ether of bisphenol-A or DGEBA) + curing agent, Epikure 3200™ (chemical name: Aminoethylpiperazine or AEP) mixture. A droplet from a sonicated suspension of MWNTs in toluene was deposited onto a Si wafer coated with a 5 nm thick layer of titanium. An individual MWNT, 85 ± 25 nm in diameter with approximately 65 shells and 10–15 μm long, hence visible under an optical microscope, was subsequently placed across the shuttles using micromanipulators housed within a probe station (The Micromanipulator Co., Carson City, NV). The embedment depth of the MWNT was measured at this point by observation of each specimen within a SEM. The uncertainties in the measurement of embedment depth arose from the pixel resolution of the SEM micrographs, which, in this case, is about 9 nm. A large droplet of epoxy (mixed with curing agent in a 10:1 ratio) was subsequently dropped onto a segment of the MWNT on one of the sample stage shuttles. The droplet upon curing (at room temperature) embedded this segment of the MWNT; the other end was "clamped" onto the device by EBID of platinum within a FIB chamber (FEI Strata DB 235, FEI corp.). The EBID process results in some Pt deposition on the exposed regions of the MWNT. However, the section of the MWNT already embedded in epoxy did not get sheathed by Pt (see Fig. 1(e)). The pullout specimen was finally post cured at 85 °C for 2 h before the pullout experiment was conducted. Note that the room temperature cure followed by post-cure was preferred over a single high temperature cure step in order to minimize the internal stresses that would develop as a result of elevated temperature cures. These stresses generally develop from shrinkage of the epoxy on polymerization or mismatch in thermal expansion coefficients between the substrate and adhesive (epoxy).

The MWNT pullout experiments were performed within a SEM (FEI Quanta 400 high resolution field emission scanning electron microscope, FEI company, Hillsboro, Oregon) equipped with an InSEM® Indenter (Agilent Technologies/Nanomechanics, Inc., Oak Ridge, Tennessee) system. A blunt Berkovich™ nanoindenter tip was used to perform the indentations. Alignment holes incorporated into the device design facilitated the alignment of the nanoindenter tip with the top shuttle of the device which ensured that the sample stage shuttles moved symmetrically. The electron beam was focused on the MWNT specimens to monitor their pullout from the epoxy matrix in real time. The experiments were conducted at an indenter tip displacement rate of 10 nm/s ($\pm$0.9 nm), and the load vs. displacement data were collected at the rate of 25 Hz. During the experiments, the maximum load applied on the device varied between 0.1 and 1 mN (load resolution of tool was about 70 nN). Once the target maximum load was reached, the load was held constant for 0.5 s. This was followed by an unloading step at the aforementioned displacement rate. During unloading, a thermal drift correction hold was conducted at about 1% of the maximum applied load for about 50 s in order to account for small amounts of thermal expansion or contraction in the test material and/or indentation equipment. Post completion of each successful pullout experiment, nanotube embedment depth was verified to ensure no breakage occurred within matrix during pullout. A SEM image showing an individual micro-device that was used to perform the pullout experiments, TEM image of an individual Mitsui™ MWNT, a representative stress-strain curve for a pristine Mitsui™ MWNT tensile specimen, AFM images used to compute RMS surface roughness values for the MWNTs, before and after fluorination, and a video showing a typical *in situ* single MWNT pullout experiment conducted within SEM have been included in the supplementary material.[31]

The MD simulations were performed using the Material Studio 6.0 software package (Material Studio 6.0 Visualizer, "Amorphous cell and Forcite Modules," Accelrys, Inc., San Diego, CA). In the simulations, a small portion of the CNT's perimeter (83 Å, viz., 5% of the perimeter of a 70 nm diameter MWNT) was modeled to be in contact with epoxy. It was assumed that the adhesion between a MWNT and epoxy was homogenous along the perimeter of the large diameter MWNT and the effects of the curvature are negligible. Hence, a flat fluorinated graphene sheet was considered for the simulations of adhesion with epoxy. The graphene model consisted of aromatic C-C bonds with a bond length of 1.42 Å and was constructed using periodic boundary conditions (PBCs). Since the goal was to compute the epoxy-graphene adhesion energies, the details of the fluorination process and changes in the hybridization of carbon atoms were not studied and only the final structure of graphene with a fluorinated surface was considered in all the simulations. The fluorine atoms were randomly dispersed on the surface of the graphene sheet. In order to study the adhesion mechanisms, the entities were built in contact in a large unit cell with a vacuum slab above the epoxy layer to remove the effects of non-bonded energy terms between different cells along the direction normal to the layers. The unit cell dimensions were $83 \times 24 \times 69$ Å. DGEBA and AEP molecules (10:1 ratio) were first packed into this unit cell with PBCs and with a density of 1.16 g/cm^3. The epoxy model was constructed using self-avoiding random-walk method of Theodorou and Suter.[28] The polymer crosslinking process was simulated using cyclic dynamic simulations in the canonical (NVT) and isothermic-isobaric ensembles (NPT) presented by Wu *et al.*[29] In this method, similar reactivity was considered for the end groups. Hydrogen atoms were removed from the end parts of DGEBA and AEP structure to provide reactive sites. In order to model the curing process, the temperature was raised to 85 °C followed by a cool down, at 20 K/100 ps, to reach room temperature. At each step of the modeling, NVT simulations were followed by NPT simulations. The Dreiding force field (FF) was used for these simulations and the total energy of the system and interface were computed.[30]

IV. CONCLUSIONS

We thus first described how a series of single nanotube pullout experiments were used to assess adhesion at the fluorinated MWNT-epoxy interface. Thirteen successful experiments allowed us to measure the average interfacial shear

strength, τ_{avg}, and the interfacial fracture energy, G_c, for the MWNT-Epon 828 interface, which were found to be significantly higher than those reported earlier for the pristine MWNT-Epon 828^{TM} system. G_c values were independently ascertained by modeling the fluorinated graphene-Epon 828^{TM} system using MD simulations. With covalent bonding and polymer chain wrapping presumably playing a limited role, if any, in interfacial adhesion, improved interfacial fracture energy values are assumed to be the result of an enhancement in the extent of interfacial nanomechanical interlocking as well as due to the electrostatic interactions between the highly electronegative fluorine atoms on MWNT surface and the epoxy matrix.

ACKNOWLEDGMENTS

Y.G., C.P., J.Z., A.C., and J.L. would like to acknowledge the support by National Science Foundation Grant No. NSF CMMI 0800896, the Welch Foundation Grant No. C-1716, and the AFOSR Grant No. FA9550-13-1-0084. H.S., N.R., and V.K. would like to acknowledge PipeWrap, LLC, for partial support. The authors would also like to thank Dr. Padraig Moloney and Dr. James Tour for providing the MWNT samples.

[1]M. Cadek, J. N. Coleman, V. Barron, K. Hedicke, and W. J. Blau, Appl. Phys. Lett. **81**, 5123 (2002).
[2]M. D. Frogley, D. Ravich, and H. D. Wagner, Compos. Sci. Technol. **63**, 1647 (2003).
[3]L. Liu and H. D. Wagner, Compos. Sci. Technol. **65**, 1861 (2005).
[4]J. Zhu, J. Kim, H. Peng, J. L. Margrave, V. N. Khabashesku, and E. V. Barrera, Nano Lett. **3**, 1107 (2003).
[5]E. T. Mickelson, I. W. Chiang, J. L. Zimmerman, P. J. Boul, J. Lozano, J. Liu, R. E. Smalley, R. H. Hauge, and J. L. Margrave, J. Phys. Chem. B **103**, 4318 (1999).
[6]J. Chen, A. M. Rao, S. Lyuksyutov, M. E. Itkis, M. A. Hamon, H. Hu, R. W. Cohn, P. C. Eklund, D. T. Colbert, R. E. Smalley, and R. C. Haddon, J. Phys. Chem. B **105**, 2525 (2001).
[7]H. Peng, L. B. Alemany, J. L. Margrave, and V. N. Khabashesku, J. Am. Chem. Soc. **125**, 15174 (2003).
[8]W. Huang, S. Fernando, L. F. Allard, and Y.-P. Sun, Nano Lett. **3**, 565 (2003).
[9]A. Hirsch, Angew. Chem., Int. Ed. **41**, 1853 (2002).
[10]D. Tasis, N. Tagmatarchis, A. Bianco, and M. Prato, Chem. Rev. **106**, 1105 (2006).
[11]L. S. Schadler, S. C. Giannaris, and P. M. Ajayan, Appl. Phys. Lett. **73**, 3842 (1998).
[12]M. S. P. Shaffer and A. H. Windle, Adv. Mater. **11**, 937 (1999).
[13]T. Ozkan, Q. Chen, and I. Chasiotis, Compos. Sci. Technol. **72**, 965 (2012).
[14]A. H. Barber, S. R. Cohen, S. Kenig, and H. D. Wagner, Compos. Sci. Technol. **64**, 2283 (2004).
[15]A. H. Barber., S. R. Cohen, A. Eitan, L. S. Schadler, and H. D. Wagner, Adv. Mater. **18**, 83 (2006).
[16]M. P. Manoharan, A. Sharma, A. V. Desai, M. A. Haque, C. E. Bakis, and K. W. Wang, Nanotechnology **20**, 295701 (2009).
[17]X. Chen, M. Zheng, C. Park, and C. Ke, Small **9**, 3345 (2013).
[18]C. Y. Yue and M. Y. Quek, J. Mater. Sci. Lett. **15**, 528 (1996).
[19]Y. Ganesan, Y. Lu, C. Peng, H. Lu, R. Ballarini, and J. Lou, J. MEMS **19**, 675 (2010).
[20]Y. Ganesan, C. Peng, Y. Lu, L. Ci, A. Srivastava, P. M. Ajayan, and J. Lou, ACS Nano **4**, 7637 (2010).
[21]Y. Ganesan, C. Peng, Y. Lu, P. E. Loya, P. Moloney, E. Barrera, B. I. Yakobson, J. M. Tour, R. Ballarini, and J. Lou, ACS Appl. Mater. Interfaces **3**, 129 (2011).
[22]H. D. Wagner, O. Lourie, Y. Feldman, and R. Tenne, Appl. Phys. Lett. **72**, 188 (1998).
[23]K. R. Jiang and L. S. Penn, Compos. Sci. Technol. **45**, 89 (1992).
[24]Y. Ganesan, C. Peng, L. Ci, V. Khabashesku, P. M. Ajayan, and J. Lou, *Fundamentals of Low-Dimensional Carbon Nanomaterials* (Mater. Res. Soc. Proc., 2011), Vol. 1284, p. 157.
[25]C. A. May, *Epoxy Resins, Chemistry and Technology* (Marcel Dekker, New York, 1988), p. 608.
[26]S. Zhandarov, E. Pisanova, E. Mäder, and J. A. Nairn, J. Adhes. Sci. Technol. **15**, 205 (2001).
[27]H. Salahshoor and N. Rahbar, J. Appl. Phys. **112**, 023510 (2012).
[28]D. N. Theodorou and U. W. Suter, Macromolecules **18**, 1467 (1985).
[29]C. Wu and W. Xu, Polymer **47**, 6004 (2006).
[30]S. L. Mayo, B. D. Olafson, and W. A. Goddard, J. Phys. Chem. **94**, 8897 (1990).
[31]See supplementary material at http://dx.doi.org/10.1063/1.4881882 for information about single fiber pullout experimental technique (includes single nanotube pullout video and SEM image of single nanotube pullout experimental setup), TEM and AFM analysis of the MWNTs and stress-strain curve for a pristine MWNT subjected to uniaxial tension.